

PAPER • OPEN ACCESS

## Search for mixed-symmetry states in $^{212}\text{Po}$

To cite this article: D. Kocheva *et al* 2016 *J. Phys.: Conf. Ser.* **724** 012023

View the [article online](#) for updates and enhancements.

### Related content

- [Description of the evolution of mixed-symmetry states in the N equals 78 isotonic chain with IBM2](#)

Zhang Da-Li, Yuan Shu-Qing and Ding Bin-Gang

- [Mixed-symmetry states in lighter odd nuclei](#)

P Van Isacker, J P Elliott and J A Evans

- [Direct Evidence for Proton-Neutron Out-of-Phase Coupling in Mixed-Symmetry States from Scattering Experiments on  \$^{92}\text{Zr}\$](#)

N Pietralla, C Walz, V Yu Ponomarev et al.

# Search for mixed-symmetry states in $^{212}\text{Po}$

D. Kocheva<sup>1</sup>, G. Rainovski<sup>1</sup>, J. Jolie<sup>2</sup>, N. Pietralla<sup>3</sup>, C. Stahl<sup>3</sup>, P. Petkov<sup>4</sup>, A. Blazhev<sup>2</sup>, A. Hennig<sup>2</sup>, A. Astier<sup>5</sup>, Th. Braunroth<sup>2</sup>, L. Cortes<sup>3</sup>, A. Dewald<sup>2</sup>, M. Djongolov<sup>1</sup>, C. Fransen<sup>2</sup>, K. Gladnishki<sup>1</sup>, V. Karayonchev<sup>2</sup>, J. Litzinger<sup>2</sup>, C. Müller-Gatermann<sup>2</sup>, M. Scheck<sup>3</sup>, Ph. Scholz<sup>2</sup>, C. Schramm<sup>2</sup>, P. Tölle<sup>2</sup>, V. Werner<sup>2</sup>, W. Witt<sup>2</sup>, D. Wölk<sup>2</sup> and P. Van Isacker<sup>6</sup>

<sup>1</sup> Faculty of Physics, St. Kliment Ohridski University of Sofia, 1164 Sofia, Bulgaria

<sup>2</sup> Institut für Kernphysik, Universität zu Köln, D-50937 Köln, Germany

<sup>3</sup> Institut für Kernphysik, Technische Universität Darmstadt, D-64289 Darmstadt, Germany

<sup>4</sup> Bulgarian Academy of Sciences, Institute for Nuclear Research and Nuclear Energy, 1784 Sofia, Bulgaria

<sup>5</sup> CSNSM, IN2P3/CNRS and Université Paris-Sud, F-91405 Orsay Campus, France

<sup>6</sup> Grand Accélérateur National d'Ions Lourds, CEA/DSM-CNRS/IN2P3, BP 55027, F-14076 Caen Cedex 5, France

E-mail: dkocheva@phys.uni-sofia.bg

**Abstract.** In this work we present an experiment dedicated to searching for quadrupole-collective isovector valence-shell excitation – the states with so-called mixed proton-neutron symmetry (MSSs), in the nucleus  $^{212}\text{Po}$ . The states of interest were populated and studied by an  $\alpha$ -transfer reaction. The experiment provides indication for existence of one-phonon MSS in the nucleus  $^{212}\text{Po}$  which is the first experimentally identified MSS in the region around double magic nucleus  $^{208}\text{Pb}$ .

## 1. Introduction

States with mixed proton-neutron symmetry (MSSs) are the lowest-lying isovector excitations in the valence shell [1] for vibrational nuclei. These states have been defined in the framework of the Interacting Boson Model with proton-neutron degrees of freedom (IBM-2), proposed by Arima and Iachello[2, 3]. The states' properties simultaneously depend on the nuclear quadrupole collectivity, the underlying single particle structure, and the proton-neutron balance of the wave function. Mixed-symmetry states can be identified experimentally by their unique decay to the low-lying fully-symmetry states (FSSs) [4]. This comprises a major challenge since it requires full spectroscopic information, i.e. the spin-parities of these non-yrast states, the lifetimes, the branching ratio and the multipole mixing ratio have to be determined. The one-phonon mixed-symmetry state decays to the  $2_1^+$  by a strong  $M1$ -transition. The best examples of MSSs are found in the regions with atomic mass around  $A \approx 90$  [5] and  $A \approx 130$  [6, 7, 8, 9, 10, 11]. The available information on MSSs in vibrational nuclei shows that good candidates for MSSs reside around double magic nuclei. Thus, the main goal of the present study is the identification of MSS in the vicinity of double magic nucleus  $^{208}\text{Pb}$ .



Content from this work may be used under the terms of the [Creative Commons Attribution 3.0 licence](#). Any further distribution of this work must maintain attribution to the author(s) and the title of the work, journal citation and DOI.

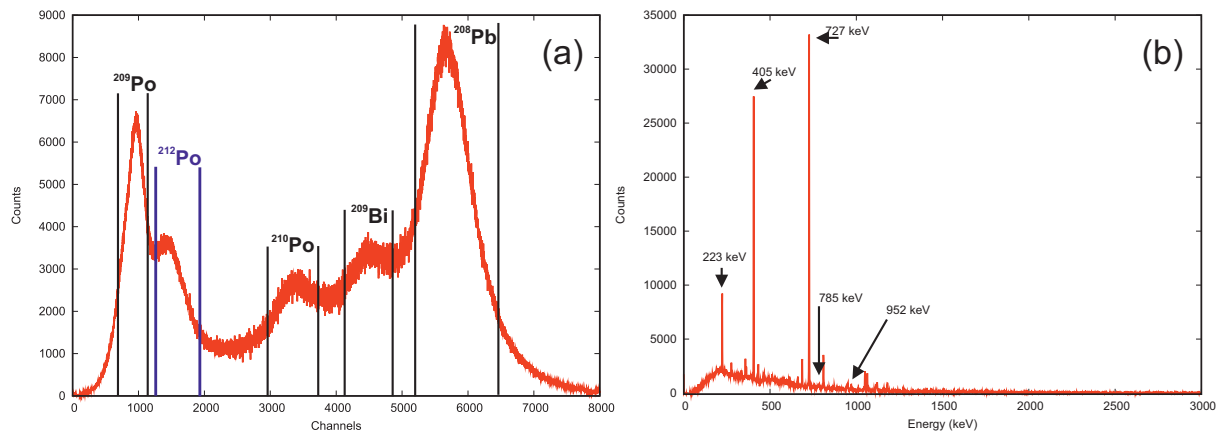


**Figure 1.** (a) The projection of the particle- $\gamma$  matrix (at  $142^\circ$ ). The vertical lines represent groups of particles found to be in coincidences with the  $\gamma$ -rays from the indicated nuclei. (b) The  $\gamma$ -ray spectrum in coincidences with the region indicated as " $^{212}\text{Po}$ " in panel (a).

## 2. Identification of the one-phonon $2^+$ mixed-symmetry state of $^{212}\text{Po}$

The experiment was performed at the FN Tandem facility of the University of Cologne, Germany. The excited states of interest were populated using the transfer reaction  $^{208}\text{Pb}(^{12}\text{C}, ^8\text{Be})^{212}\text{Po}$ . The beam was accelerated to 62 MeV which is about 2 MeV below the Coulomb barrier. The target was a self-supporting 10 mg/cm<sup>2</sup> thick Pb foil enriched up to 99.14% with the isotope  $^{208}\text{Pb}$ . The reaction took place in the reaction chamber of the Cologne coincidence plunger device [12]. To detect the light reaction fragments six solar cells (10 mm  $\times$  10 mm) were used. The array of solar cells was mounted at backward angles with respect to the beam axis, covering an annular space between  $116.8^\circ$  and  $167.2^\circ$ . The solar cells were placed at a distance of about 15 mm between their centers and the target.

The emitted gamma-rays were registered by 12 HPGe detectors mounted outside the plunger chamber in three rings at, on average, 12 cm from the target. Five detectors were positioned at backward angles ( $142.3^\circ$  with respect to the beam axes). Six detectors were placed at forward angles ( $35^\circ$ ) and a single detector was positioned at  $0^\circ$ . The master trigger was set for at least one particle (signal in the solar cells) and one  $\gamma$ -ray (signal in the HPGe detector) or at least two  $\gamma$ -rays. The particle- $\gamma$  coincidence data was sorted in three matrices with respect to the angular position of the HPGe detectors.

In Fig. 1(a) is shown the projection of the particle- $\gamma$  matrix. Note that the actual counts correspond to the fragments (ejectiles) from the transfer reactions. For instance, the  $\gamma$ -spectrum of  $^{212}\text{Po}$  (shown in Fig. 1(b)) is in coincidence with  $^8\text{Be}$  (or 2  $\alpha$ -particles). This spectrum is dominated by the 727-keV, the 405-keV and the 223-keV lines which are the transitions from the first three yrast states in  $^{212}\text{Po}$  [13]. Besides some contaminants from  $^{211}\text{Po}$  all other  $\gamma$  lines in the spectrum in Fig. 1(b) also originated from the decay of excited states in  $^{212}\text{Po}$ .

A partial level scheme of the states in  $^{212}\text{Po}$  populated in the present experiment was constructed on the basis of the  $\gamma$ - $\gamma$  coincidence relationships. The level scheme is shown in Fig. 2. The levels are observed in another  $\alpha$ -transfer reaction, namely  $^{208}\text{Pb}(^{18}\text{O}, ^{14}\text{C})^{212}\text{Po}$  [13] but we have also populated two non-yrast  $2^+$  states at excitation energies at 1512 keV and at 1679 keV, respectively [14]. Taking into account the branching ratio and the multipole mixing ratio of these two levels (+0.09(3) and +0.65(50) [14], respectively) these states show a predominant  $M1$ -transition to the  $2_1^+$  state via the 785-keV and the 952-keV, respectively [18]. That makes these two  $2^+$  states potential candidates for the one-phonon MSS in  $^{212}\text{Po}$ . The only missing piece of experimental information that is needed for identification of these states

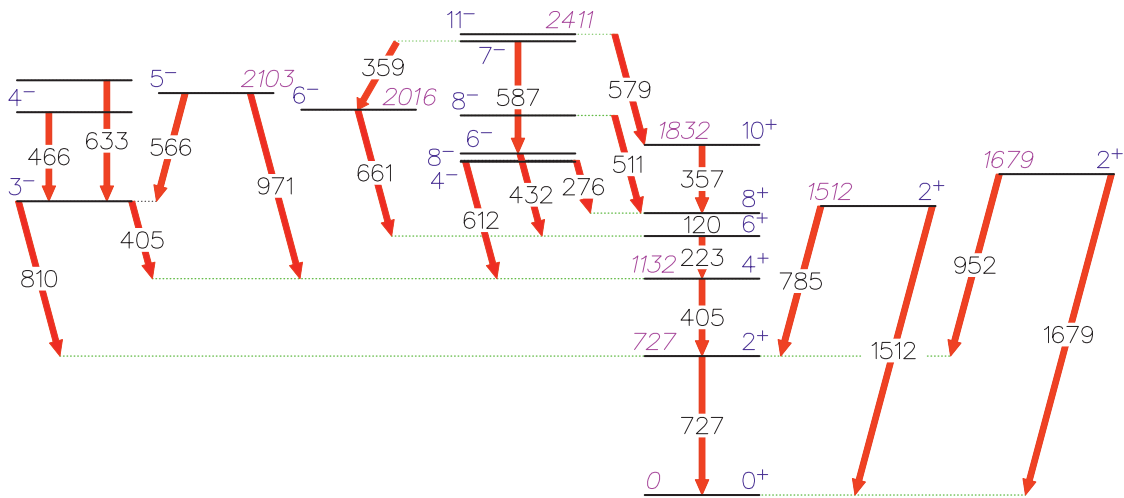


**Figure 2.** Partial level scheme of  $^{212}\text{Po}$  obtained in the present work. For the spin and parity quantum numbers we have adopted the values reported in the previous studies [13, 14, 15, 16, 17]. The energy of the transitions are given in keV. The candidates for the one-phonon MSS are placed on the right of the yrast states.

as MSSs are short lifetimes. The determination of these lifetimes is possible by means of the Doppler Shift Attenuation Method (DSAM) (cf. Ref. [19] and references therein) due to the well pronounced Doppler shapes in both lines of interest.

For extracting the lifetimes two parallel analyses were used. The first one, labelled here Analysis I, is based on a Monte Carlo (MC) simulation by means of a modified [20, 21] version of the program DESASTOP [22] in order to describe the slowing down of the recoiling nuclei. The electronic stopping powers are taken from the Northcliffe and Schilling tables [23] with corrections for the atomic structure of the medium, as discussed in Ref. [24]. An empirical reduction of  $f_n = 0.7$  was applied [25] to downscale the nuclear stopping power predicted by the theory of Lindhard, Scharff, and Schitt [26]. In the second analysis, labelled here Analysis II, an integrated software named APCAD (Analysis Program for Continuous Angle DSAM) is used [27]. In APCAD, the slowing down process is simulated by GEANT4 [28] as the electronic stopping process is modelled in the same way as in Analysis I. On the other side, APCAD adopts a simpler approach to modelling the nuclear stopping process, compared to the completely discrete approach used in Analysis I; in Analysis II the angular straggling due to nuclear collisions is modelled discretely by means of MC simulation while the corresponding energy loss is considered to emerge as a result from a continuous process and the nuclear stopping powers were taken from SRIM2013 [29] and reduced by 40%. Both analyses take into account the response of the HPGe detectors, the experimental geometry and the restrictions on the reaction kinematics imposed by the solar cells array. The feeding histories of the levels of interest were determined by the  $\gamma-\gamma$  coincidence data. Slow feeding was introduced and fitted in the analyses only if the analysed transitions were observed in coincidence with transitions from higher-lying states. In the opposite case, only very fast feeding which can be associated with direct population of the levels of interest, was considered. Under these assumptions both analyses produced similar results for the level at 2016 keV in  $^{212}\text{Po}$  (see Table 1).

For extracting the lifetime from the lineshape of the 661.3-keV transition a feeding history similar to the one used in Ref. [13] (58% fast feeding and 42% slow feeding) is used (see Table 1). The lifetimes of the  $2_2^+$  state at 1512 keV and  $2_3^+$  state at 1679 keV were extracted from the lineshapes of the transitions  $E_\gamma = 785$  keV and  $E_\gamma = 952$  keV, respectively. Both of these

**Table 1.** The results for the lifetime of the  $6^-$  state at 2016 keV (see Fig. 2) extracted by both parallel analyses.

	Ref. analysis [17]	Analysis 1	Analysis 2
$\tau(ps)$	0.49(16)	0.50(4)	0.47(3)

**Table 2.** Properties of the  $2_2^+$  and the  $2_3^+$  states of  $^{212}\text{Po}$ . The results for the lifetimes and the transitions strengths are preliminary.

$E_{level}(\text{keV})$	$J^\pi$	$\tau(ps)$ <sup>0</sup>	$E_\gamma(\text{keV})$	$I_\gamma$ , Ref. [18]	$\alpha$ , Ref. [18]	$J_{final}^\pi$	$\delta$ , Ref. [14]	Transition strength <sup>1</sup> $B(E2)$ in $e^2\text{fm}^4$ ; $B(M1)$ in $\mu_N^2$
1512	$2_2^+$	0.67(5)	1512.7	26(3)		$0_1^+$		$B(E2)=32(4)$
			785.4	100(1)	0.0408(2)	$2_1^+$	0.09(3)	$B(M1)=0.133(9)$ $B(E2)=25(16)$
1679	$2_3^+$	0.68(2)	1679.7	35(8)		$0_1^+$		$B(E2)=23(5)$
			952.1	100(19)	0.020(5)	$2_1^+$	0.65(50)	$B(M1)=0.049(17)$ $B(E2)=331(306)$

<sup>0</sup> From the present experiment. Preliminarily results.

<sup>1</sup> From the present experiment. Preliminarily results.

transitions are in coincidence with 727-keV transition, only. As a result only fast feeding was considered. The preliminary results for the lifetimes together with the available spectroscopic information and the resulting transition strengths are summarized in Table 2. The  $2_2^+$  state in  $^{212}\text{Po}$  at 1512 keV excitation energy decays with a sizeable  $M1$ -transition to the  $2_1^+$  state. This allows us to conclude that the  $2_2^+$  state in  $^{212}\text{Po}$  is, at least, a fragment of the one-phonon MSS.

### 3. The spectrum of $^{212}\text{Po}$ from a simple perspective

The nucleus  $^{212}\text{Po}$  has two protons and two neutrons outside the core of  $^{208}\text{Pb}$ . In the simplest approach the neutrons are in the  $2g_{9/2}$  orbital and the protons – in  $1h_{9/2}$ . States with two neutrons in the  $2g_{9/2}$  orbital and two protons in the  $1h_{9/2}$  orbital can be described in the basis

$$|(2g_{9/2})^2 J_\nu, (1h_{9/2})^2 J_\pi; J\rangle \equiv |J_\nu J_\pi J\rangle \quad (1)$$

The neutron-neutron and proton-proton interactions are diagonal in this basis which is mixed by the neutron-proton interaction

$$\begin{aligned} \langle J_\nu J_\pi J | \hat{H} | J'_\nu J'_\pi J' \rangle &= (V_{\nu\nu}^{J_\nu} + V_{\pi\pi}^{J_\pi}) \delta_{J_\nu J'_\nu} \delta_{J_\pi J'_\pi} + \\ &+ 4\sqrt{(2J_\nu + 1)(2J_\pi + 1)(2J'_\nu + 1)(2J'_\pi + 1)} \times \sum_R (2R + 1) \begin{bmatrix} j_\nu & j_\pi & J_\pi & J_\nu \\ & R & j_\pi & J & j_\nu \\ j_\nu & j_\pi & J'_\pi & J'_\nu \end{bmatrix} V_{\nu\pi}^R \end{aligned} \quad (2)$$

where  $V_{\nu\nu}^{J_\nu}$ ,  $V_{\pi\pi}^{J_\pi}$  and  $V_{\nu\pi}^R$  are the neutron-neutron, proton-proton and neutron-proton interaction matrix elements, respectively, and the symbol in square brackets is a  $12j$  coefficient [30]. These three interactions are taken from the energy spectra of the neighbouring nuclei with neutrons and protons in the required shell configurations. In particular, in the single-shell approximation

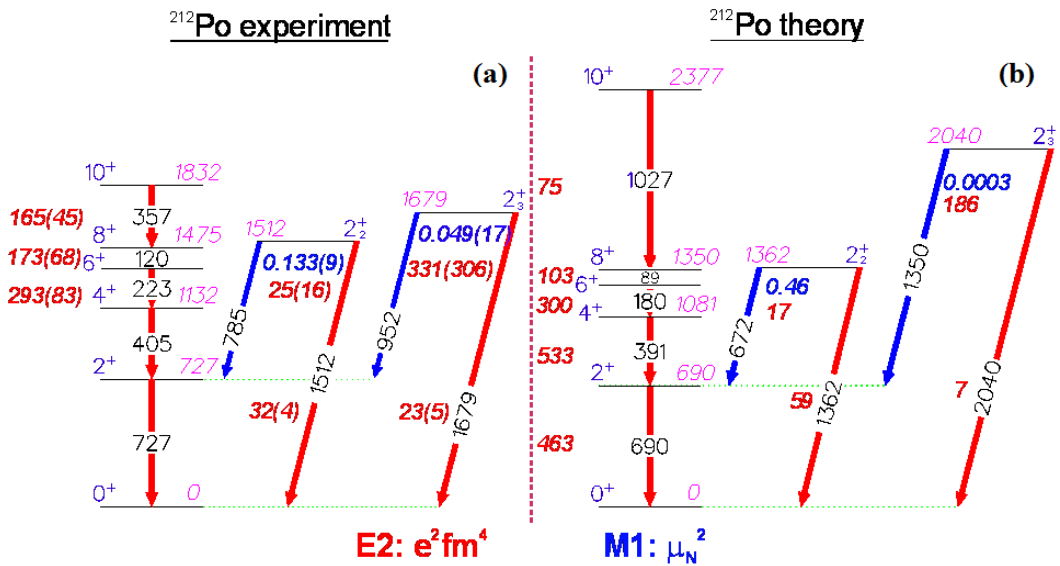


**Figure 3.** (a) The part of the experimental spectrum of  $^{212}\text{Po}$  representing the yrast states and the levels of interest. (b) The calculated (for details see the text) yrast states and the two lowest  $2^+$  energy levels of  $^{212}\text{Po}$ .

$^{210}\text{Pb}$  corresponds to two neutrons in the  $2g_{9/2}$  orbital and  $^{210}\text{Po}$  to two protons in  $1h_{9/2}$ . Both of these nuclei display seniority-like spectra. The interaction between a neutron in the  $2g_{9/2}$  orbital and a proton in the  $1h_{9/2}$  orbital can be determined by the energy spectrum of  $^{210}\text{Bi}$ .

In the single-shell approximation the  $M1$  operator can be determined by the magnetic moments of the ground states of  $^{209}\text{Pb}$  and  $^{209}\text{Bi}$  –  $\mu(9/2_1^+) = -1.4735 \mu_N$  and  $\mu(9/2_1^-) = +4.1103 \mu_N$ . This yields an effective neutron  $g$  factor of  $g_\nu = -0.33 \mu_N$  and an effective proton  $g$  factor of  $g_\pi = +0.91 \mu_N$ . The  $M1$  operator can be written as

$$\hat{T}_\mu(M1) = \sqrt{\frac{3}{4\pi}} \sqrt{\frac{j(j+1)(2j+1)}{3}} [g_\nu(\nu_j^+ \times \tilde{\nu}_j)_\mu^{(1)} + g_\pi(\pi_j^+ \times \tilde{\pi}_j)_\mu^{(1)}], \quad (3)$$

where  $\nu_j^+$  and  $\pi_j^+$  are the neutron and proton create operators in the  $j$  orbital (here  $j = j_\nu = j_\pi = 9/2$ ) and  $\tilde{\nu}_{jm} = (-)^{j+m} \nu_{j-m}$  ( $\tilde{\pi}_{jm} = (-)^{j+m} \pi_{j-m}$ ).

The  $E2$  operator can be determined by the nuclei  $^{210}\text{Pb}$  and  $^{210}\text{Po}$  due to the pure two-nucleon configurations in  $8_1^+$  and  $6_1^+$  states in these nuclei. Therefore, the effective charges of  $e_\nu = 0.88$  and  $e_\pi = 1.11$  are derived from the transition  $B(E2; 8^+ \rightarrow 6^+)$ . The form of the  $E2$  operator is

$$\hat{T}_\mu(E2) = -\sqrt{\frac{(2j-1)(2j+1)(2j+3)}{64\pi j(j+1)}} \left( N + \frac{3}{2} \right) b^2 [e_\nu(\nu_j^+ \times \tilde{\nu}_j)_\mu^{(2)} + e_\pi(\pi_j^+ \times \tilde{\pi}_j)_\mu^{(2)}], \quad (4)$$

where  $N$  is the major oscillation quantum number and  $b$  is the length parameter of the oscillator,  $b \approx 1.0A^{1/6}$  fm. With this information an empirical description of the nucleus  $^{212}\text{Po}$  is possible. The results from the calculations are compared to the experimental ones in Fig. 3.

Both schemes in Fig. 3(a) and 3(b) show a qualitative agreement, except for the  $10_1^+$  and the  $2_3^+$  states. The similar behaviour is valid for transition strengths, too.

Of particular interest is to examine the wave functions' structures of the  $2^+$  states. There are twelve different ways to couple all possible  $J_\nu$  with all possible  $J_\pi$  to total angular momentum  $J = 2$ . The two lowest energy levels can be described by the following wave functions:

$$\begin{aligned} |2_1^+\rangle &= 0.448|J_\nu = 0, J_\pi = 2, J = 2\rangle + 0.819|J_\nu = 2, J_\pi = 0, J = 2\rangle + \dots \\ |2_2^+\rangle &= 0.813|J_\nu = 0, J_\pi = 2, J = 2\rangle - 0.517|J_\nu = 2, J_\pi = 0, J = 2\rangle + \dots \end{aligned} \quad (5)$$

In both cases the two components define a good fraction of the entire state (87% and 93%, respectively) and define almost mutually orthogonal states. Therefore, the first excited two  $2^+$  states can be analyzed in terms of the components of proton and neutron S ( $J = 0$ ) and D ( $J = 2$ ) pairs. The opposite signs in both wave functions indicate that the second  $2^+$  state is of isovector nature, in agreement with the experimentally observed sizeable  $M1$  transition between the  $2_2^+$  and the  $2_1^+$ .

The third  $2^+$  state has an entirely different structure. Its wave function can be written as

$$\begin{aligned} |2_3^+\rangle &= 0.772|J_\nu = 2, J_\pi = 2, J = 2\rangle + 0.401|J_\nu = 4, J_\pi = 4, J = 2\rangle + \\ &\quad 0.307|J_\nu = 6, J_\pi = 6, J = 2\rangle + 0.242|J_\nu = 8, J_\pi = 8, J = 2\rangle + \dots \end{aligned} \quad (6)$$

This state cannot be described in IBM-2 since it invokes pairs of all multipolarities, not only S and D.

#### 4. Conclusions

In summary, we have presented an experiment dedicated to searching of the one-phonon mixed-symmetry state in  $^{212}\text{Po}$  which is in the vicinity of the double magic nucleus  $^{208}\text{Pb}$ . The preliminary results from this investigation provide indication for the existence of this state that is the first experimentally identified one-phonon MSS in the region with atomic mass  $A \approx 208$ .

#### Acknowledgments

D.K. acknowledges the support from SF of University of Sofia under contract №152/2015. G.R. acknowledges the support from the Alexander von Humboldt foundation. This work was supported by the partnership agreement between the University of Cologne and University of Sofia, by the DAAD German-Bulgarian exchange program under grants No. PPP57082997 and No. DNTS/01/05/2014, by the DFG under grant Pi393/2-3, and by the BMBF under grants 05P12RDCI8 and 05P15RDCIA.

#### References

- [1] N. Lo Iudice and F. Palumbo, Phys. Rev. Lett. **41**, 1532 (1978).
- [2] F. Iachello, Phys. Rev. Lett. **53**, 1427 (1984).
- [3] F. Iachello and A. Arima, *The interacting boson model* (Cambridge University Press, Cambridge, 1987).
- [4] N. Pietralla, P. von Brentano, A.F. Lisetskiy, Prog. Part. Nucl. Phys. **60**, 225 (2008) and the references therein.
- [5] K. Heyde, P. von Neumann-Cosel, A. Richter, Rev. Mod. Phys. **82**, 2366 (2010).
- [6] G. Rainovski *et al.*, Phys. Rev. Lett. **96**, 122501 (2006).
- [7] T. Ahn *et al.*, Phys. Lett. **B679**, 19 (2009).
- [8] L. Coquard *et al.*, Phys. Rev. C **82**, 024317 (2010).
- [9] K.A. Gladnishki *et al.*, Phys. Rev. C **82**, 037302 (2010).
- [10] M. Danchev *et al.*, Phys. Rev. C **84**, 061306(R) (2011).
- [11] T. Ahn *et al.*, Phys. Rev. C **86**, 014303 (2012).
- [12] A. Dewald, O. Möller, P. Petkov, Prog. Part. Nucl. Phys. **67**, 786 (2012).
- [13] A. Astier, P. Petkov, M.-G. Porquet, D. S. Delion, and P. Schuck, Phys. Rev. Lett. **104**, 042701 (2010); A. Astier, P. Petkov, M.-G. Porquet, D. S. Delion, and P. Schuck, Eur. Phys. J. A **46**, 165 (2010).

- [14] B. Bengtson *et al.*, Nucl. Phys. A **378**, 1 (1982).
- [15] A.R. Poletti *et al.*, Nucl. Phys. A **473**, 595 (1987).
- [16] Zs. Podolýak *et al.*, Nucl. Instrum. Methods Phys. Res. A **511**, 354 (2003).
- [17] A.B. Garnsworthy *et al.*, J. Phys. G **31**, S1851 (2005).
- [18] E. Browne, Nuclear Data Sheets **104**, 427 (2005).
- [19] T. K. Alexander and J. S. Forster, Adv. Nucl. Phys. **10**, 197 (1978).
- [20] P. Petkov *et al.*, Nucl. Phys. A **640**, 293 (1998).
- [21] P. Petkov *et al.*, Nucl. Instrum. Methods Phys. Res. A **431**, 208 (1999).
- [22] G. Winter, ZfK. Rossendorf Report ZfK-497, 1983; G. Winter, Nucl. Instrum. Methods **214**, 537 (1983).
- [23] L. C. Northcliffe and R. F. Schilling, Nucl. Data Sect. **7**, 233 (1970).
- [24] J. F. Ziegler and J. P. Biersack, in *Treatise on Heavy Ion Science*, edited by D. A. Bromley (Plenum Press, New York, 1985), Vol. 6, p. 95.
- [25] J. Keinonen, AIP Conf. Proc. **125**, 557 (1985).
- [26] J. Lindhard, M. Scharff, and H. E. Schitt, Kgl. Dan. Vid. Selsk. Mat. Fys. Medd. **33**, 14 (1963).
- [27] C. Stahl, PhD thesis, TU Darmstadt (2015).
- [28] S. Agostinelli *et al.*, Nucl. Instrum. Methods Phys. Res. A **506**, 250 (2003).
- [29] J.F. Ziegler, M.D. Ziegler, J.P. Biersack, Nucl. Instr Meth., B **268**, 1823 (2010).
- [30] A.P. Yutsis, I.B. Levinson and V.V. Vanagas, *The theory of angular momentum* (Israel Program for Scientific Translations, Jerusalem, 1962).